Lattice electrical resistivity of magnetic bcc iron from first-principles calculations

Dario Alfè,[1,*] Monica Pozzo,[1] and Michael P. Desjarlais[2]

[1]*Department of Earth Sciences, Department of Physics and Astronomy, London Centre for Nanotechnology and Thomas Young Centre @UCL, University College London, Gower Street, London WC1E 6BT, United Kingdom*

[2]*Pulsed power Sciences Center, Sandia National Laboratories, Albuquerque, New Mexico 87185, USA*

(Received 6 October 2011; published 6 January 2012)

We have calculated the lattice contribution to the electrical resistivity of body-centered-cubic iron at ambient pressure and two temperatures, 300 K and 500 K, using density functional theory and the Kubo-Greenwood formula. We performed extensive size and **k**-point sampling tests by including up to 1024-atom cells and up to 10 **k** points. The calculated resistivities fall within the range of the experimental estimates at 500 K, and overestimate it by only ∼5% at 300 K.

DOI: 10.1103/PhysRevB.85.024102 PACS number(s): 72.15.Cz, 71.15.−m, 65.20.−w

I. INTRODUCTION

Iron is the most abundant metal in the solar system, and believed to be the main constituent of the Earth's core.[1] For this reason, it is very important to understand the thermophysical properties of iron, in particular at the conditions of high pressure (p) and high temperature (T) found in the Earth's interior. The development of high performance computers and modern theoretical methods based on density functional theory[2] have made it possible to compute many properties of iron, including the zero temperature transition pressure from the body-centered-cubic (bcc) to the hexagonal-closed-packed (hcp) structure, the bcc structural properties, magnetic moment, and the phonon spectrum.[3–6] High pressure-high temperature properties have also been computed with DFT, including crystal structure stability,[7] the viscosity of the liquid,[8,9] and the iron melting curve.[10–12] For the latter, there have also been recent attempts to go beyond DFT with highly accurate quantum Monte Carlo methods.[13,14] However, so far little has been done on the iron transport properties, particularly in the high p,T region,[15] despite its great importance to determine the amount of heat transfer in the Earth's core, and what remains available to drive the geodynamo for the generation of the Earth's magnetic field.

The first-principles calculation of the electrical resistivity of metals, based on the Kubo-Greenwood formula,[16,17] has been recently successfully carried out for various systems, including, for example, Na,[18–20] Al,[21–23] He,[24] H,[25] mixtures of Be, C, D, and T,[26] and water.[27] -In this paper, we are interested in the electrical resistivity of iron, and in particular in testing the accuracy of DFT with the Perdew-Wang (PW91) functional.[28] Our general aim is to establish the reliability of DFT-PW91 at zero pressure, and then use it in a work to follow to compute the resistivity of iron and iron alloys at Earth's core conditions.

Iron at ambient conditions has an additional complication that is not present at high pressure and high temperature: it is magnetic. In fact, any calculation for bcc iron at low pressure needs to include magnetism, otherwise the crystal is unstable (some phonon frequencies are imaginary if magnetism is neglected). Moreover, a calculation of the total resistivity would need to include the noncollinearity of the spins.[29] However, it is well known that the electrical resistivity of magnetic metals can be separated into a lattice contribution ρ_l due to thermal vibrations, plus a magnetic contribution ρ_m due to spin disorder and the excitation of spin waves. The latter is thought to be mainly caused by the scattering of the itinerant s electrons by the more localized d orbitals via s-d exchange interaction.[30,31] The lattice contribution is roughly proportional to temperature above the Debye temperature, while the magnetic contribution grows as T^3,[31] and for iron it becomes the dominant contribution before saturation at the Curie temperature. To estimate the lattice contribution ρ_l and the magnetic contribution ρ_m from a measurement of the total resistivity, Weiss and Marotta[32] assumed a linear behavior of ρ_l with T, and obtained the slope by fitting the resistivity data above the Curie temperature, where ρ_m is constant. The behavior of ρ_m is then obtained by subtracting ρ_l from the total resistivity. A similar procedure was also adopted by Bäcklund,[33] who obtained similar results, and found that at 300 K the lattice contribution ρ_l is ∼80% of the total resistivity, reducing to ∼60% of the total at 500 K.

Here we use collinear spin-polarized DFT-PW91 to calculate the electrical resistivity of solid bcc Fe at zero pressure and at 300 and 500 K, using the Kubo-Greenwood[16,17] formula. Because of the collinearity of the spins, the magnetic contribution to the resistivity is largely absent, and therefore the calculations should be compared with the lattice component of the resistivity. We carefully address the issue of simulation cell size and **k**-point sampling, showing that at low temperature significantly large simulation cells are required to converge the results. Agreement with experimental estimates of the lattice resistivity is good. In Sec. II, we describe the method and the computational framework. The results are presented in Sec. III, followed by our conclusions in Sec. IV.

II. TECHNIQUES

First-principles simulations were performed using the VASP code,[34] with the projector augmented wave (PAW) method[35,36] and the Perdew-Wang[28] functional, fully including spin polarization. We tested the parametrization of the exchange-correlation functional of Perdew-Zunger[37](PZ) or Vosko-Wilk-Nusair,[38] which showed no appreciable differences between the two schemes, and we therefore chose to use the PZ parametrization. Most calculations were performed with an

Fe PAW with only the $4s$ and $3d$ electron in valence. We also tested the effect of including the $3s$ and $3p$ electrons in valence, which affect the optical spectrum in the high energy region, but have an undetectable effect on the electrical conductivity (the inverse of the electrical resistivity). Single particle orbitals were expanded in plane waves with a cutoff of 293.3 and 547.3 eV for the PAW's with the $4s^1 3d^7$ and $3s^2 sp^6 4s^1 3d^7$ valence configurations respectively, and the core radii were 1.16 and 0.85 Å, respectively. Electronic levels were occupied according to Fermi-Dirac statistics, with an electronic temperature corresponding to the temperature of the system. An efficient extrapolation of the charge density was used to speed up the *ab initio* molecular dynamics simulations,[39] which were performed by sampling the Brillouin zone (BZ) with the Γ point only, and at the experimental room temperature density. The temperature was controlled with an Andersen thermostat[40] and the time step was set to 2 fs. We used simulation cells including 64, 128, 250, 432, 686, and 1024 atoms. We ran simulations for typically 3 ps, from which we discarded the first ps to allow for equilibration, and we used the last 2 ps to extract $N = 10$ configurations $\{R_I; I = 1,N\}$ equally spaced in time. These N configurations were then used to compute the electrical conductivity via the Kubo-Greenwood formula as implemented in VASP.[22]

The Kubo-Greenwood formula for the electrical conductivity as a function of frequency ω for a particular $\mathbf{k}$ point in the BZ of the simulation supercell and for a particular configuration of the ions $\{R_I\}$ reads

$$\sigma_{\mathbf{k}}(\omega; R_I) = \frac{2\pi e^2\hbar^2}{3m^2\omega\Omega}\sum_{i,j=1}^{n}\sum_{\alpha=1}^{3}[F(\epsilon_{i,\mathbf{k}}) - F(\epsilon_{j,\mathbf{k}})] \times |\langle\Psi_{j,\mathbf{k}}|\nabla_\alpha|\Psi_{i,\mathbf{k}}\rangle|^2\delta(\epsilon_{j,\mathbf{k}} - \epsilon_{i,\mathbf{k}} - \hbar\omega), \quad (1)$$

where e and m are the electron charge and mass respectively, $\hbar$ is the Plank's constant divided by 2π, Ω is the volume of the simulation cell, and n is the number of Kohn-Sham states. The α sum runs over the three spatial directions, which in bcc iron are all equivalent. $\Psi_{i,\mathbf{k}}$ is the Kohn-Sham wave function corresponding to eigenvalue $\epsilon_{i,\mathbf{k}}$, and $F(\epsilon_{i,\mathbf{k}})$ is the Fermi weight. The δ function is represented by a Gaussian, with a width chosen to be roughly equal to the average spacing between the eigenvalues weighted by the corresponding change in the Fermi function.[22] The width was chosen to be 16, 8, 4, 2.4, 2, and 1.4 meV for the, 64-, 128-, 250-, 432-, 686-, and 1024-atom systems, respectively. Integration over the BZ is performed using standard methods,[41] and the frequency dependent conductivity of the high temperature solid is obtained by averaging over the N configurations $\{R_I; I = 1,N\}$:

$$\sigma(\omega) = \frac{1}{N}\sum_{I=1}^{N}\sum_{\mathbf{k}}\sigma_{\mathbf{k}}(\omega; R_I)W(\mathbf{k}). \quad (2)$$

Here $W(\mathbf{k})$ is the weighting factor for the point $\mathbf{k}$. In principle, all the $W(\mathbf{k})$ would be identical for a simulation with no symmetries like that of a high temperature solid in a cubic box. In practice, we found it convenient to use $\mathbf{k}$ points drawn from the irreducible wedge of the BZ (IBZ) of the same system in which the atoms occupy bcc perfect lattice positions, as convergence with respect to the number of $\mathbf{k}$ points is faster if the points are chosen in this way, provided one averages over the three Cartesian directions. For example, a $4 \times 4 \times 4$ grid would yield 32 $\mathbf{k}$ points for the high temperature solid, but only 4 $\mathbf{k}$ points for the same system with full cubic symmetry. We have explicitly calculated the conductivity using both the 32- and the 4-$\mathbf{k}$-point sets for the 128 atoms system at 500 K, and verified that the two sets of calculations yield identical conductivities when averaged over time.

The dc conductivity σ_0 is given by the value of $\sigma(\omega)$ in the limit $\omega \to 0$. This limit needs to be taken with care, because at very small values of ω the conductivity falls unphysically to zero due to the artificial finite spacing between the Kohn-Sham eigenvalues, caused by the finite size of the simulation cell. To take this limit, our procedure is to fit the conductivity to a smooth function, without including in the fit values of $\sigma(\omega)$ that have started to fall to zero. Although Fe is far from being a simple metal, and a Drude model would not be appropriate to describe its optical conductivity, we found that by including a sufficiently restricted set of data, a fit to a Drude model $\sigma(\omega) = \sigma_0/(1 + \omega^2\tau^2)$ in the low energy region of the spectrum provided a convenient way to obtain the dc conductivity σ_0 and from this the resistivity $\rho = 1/\sigma_0$.

The optical conductivity must obey the sum rule

$$S = \frac{2m\Omega}{\pi e^2 N_e}\int_0^\infty \sigma(\omega)d\omega = 1, \quad (3)$$

where N_e is the number of electrons in the simulation cell. The value of S provides a useful check of the quality of the data, but in the case of iron states up to ∼150 eV above the Fermi energy must be included to satisfy the sum rule. This means that, especially for large systems, checking the validity of the sum rule can become prohibitively expensive. However, the dc conductivity is only affected by states in a window around the Fermi energy which is comparable to $k_B T$. We therefore checked the sum rule for a few configurations on the 128-atom system by including states up to 150 eV above the Fermi energy, but then for the rest of the calculations we decided to include only states up to ∼3 eV above the Fermi energy.

III. RESULTS

In Fig. 1, we show $\sigma(\omega)$ computed with the 128-atom system and the Baldereschi point[42] at the temperature of 500 K. The graph shows that $\sigma(\omega)$ is quite structured, and decays to zero only at very large energies. The sum rule for this set of data is 0.97, which indicates that the calculations are well converged. To calculate the sum rule accurately, we needed to include 10,000 bands instead of the ∼800 required to converge a standard spin-polarized calculation. However, the low energy spectrum (shown in the figure's inset) is unaffected by the high energy bands, and therefore production runs have only been done using 800 bands, which include states up to ∼3 eV above the Fermi energy. For the simulations performed with the larger cells, we have used a corresponding number of bands to include states up to ∼3 eV above the Fermi energy.

In Fig. 2, we show ρ at 500 K as a function of cell size, for various sets of $\mathbf{k}$ points, and we compare with experimental estimates. It is clear that cells including at least 250 atoms are needed for the results to be of useful accuracy, and it is also

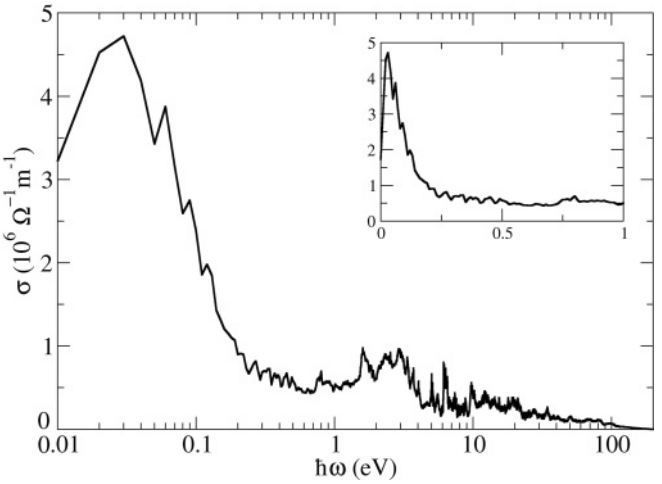

FIG. 1. Optical conductivity of bcc iron at 500 K computed using a 128-atom cell and the Baldereschi point. The calculations were performed including 10 000 single particle orbitals which extend to over 150 eV above the Fermi energy. Inset shows the low energy region of the spectrum for $0 \leqslant \hbar\omega \leqslant 1$ eV.

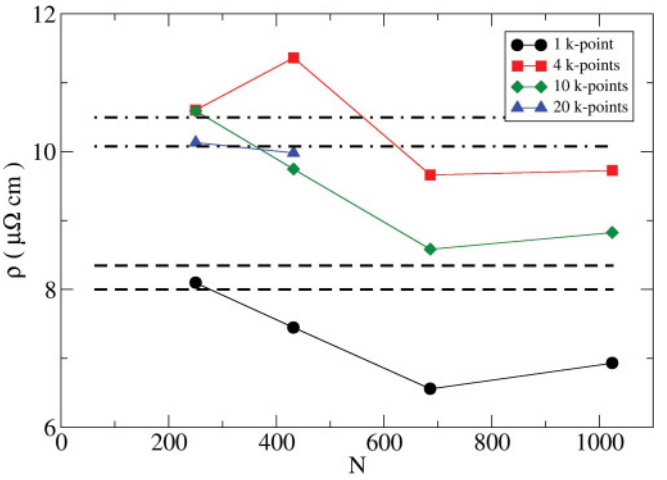

FIG. 3. (Color online) Lattice contribution to the electrical resistivity of bcc iron at 300 K, calculated using collinear spin-polarized DFT-PW91 with various cell sizes (N) and **k**-point sampling (symbols), and experimental estimates (dashed lines) by Weiss and Marotta (Ref. 32) and Bäcklund (Ref. 33). Also shown is the total measured resistivity (dot-dashed lines) (Refs. 32 and 33).

obvious that one **k** point only is not sufficient, not even for the largest 686-atom system. However, provided at least 4 **k** points are used, the results are well converged, and fall within the experimental range of estimates.

Figure 3 shows the calculated value of ρ at 300 K as a function of cell size, and for various sets of **k** points. Convergence with respect to simulation cell size and **k**-point sampling is slower at this lower temperature, as expected, because the number of states that contribute to the conductivity is roughly inversely proportional to the temperature, and therefore large cells are required at low temperatures.[20] Even with 432-atom cells the error due to convergence is still ∼10%.

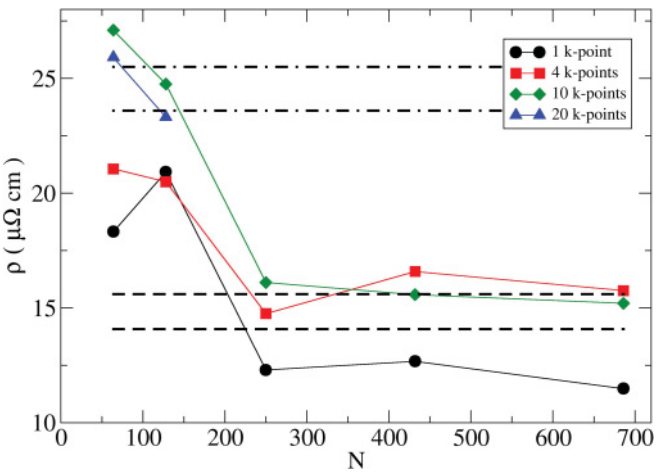

FIG. 2. (Color online) Lattice contribution to the electrical resistivity of bcc iron at 500 K, calculated using collinear spin-polarized DFT-PW91 with various cell sizes (N) and **k**-point sampling (symbols), and experimental estimates (dashed lines) by Weiss and Marotta (Ref. 32) and Bäcklund (Ref. 33). Also shown is the total measured resistivity (dot-dashed lines) (Refs. 32 and 33).

In fact, it may also be possible that the results obtained with the largest system including 1024 atoms are not completely converged, as suggested by the difference between the calculations with 4 and 10 **k** points. However, the results overestimate the resistivity only by ∼5%, and therefore the agreement with experiments is quite respectable even in this more difficult case of $T = 300$ K.

IV. CONCLUSIONS

We have computed the lattice contribution to the electrical resistivity of magnetic bcc iron at ambient pressure and two temperatures, 300 and 500 K, using collinear spin-polarized density functional theory with the PW91 functional. Extensive size and **k**-point tests showed that relatively large simulations cells are required to converge the results, particularly for the calculations at the lower temperature for which even the largest systems, including 1024 atoms, show that convergence may not have been completely achieved. The calculations overestimate the resistivity only slightly at 300 K (by ∼5%), but at 500 K our results fall within the experimental range of estimates. This work lays the foundations for a more extensive study of the resistivity of iron and iron alloys at Earth's core conditions.

ACKNOWLEDGMENTS

The work of MP and DA was conducted as part of a EURYI scheme award as provided by EPSRC (see www.esf.org/euryi), and was also supported by a NERC Grant No. NE/H02462X/1. Calculations were performed on the HECToR service in the UK and also on Legion at UCL as provided by research computing.

*d.alfe@ucl.ac.uk

[1] F. Birch, J. Geophys. Res. **57**, 227 (1952).

[2] P. Hohenberg and W. Kohn, Phys. Rev. **136**, B864 (1964); W. Kohn and L. Sham, *ibid.* **140**, A1133 (1965).

[3] L. Stixrude, R. E. Cohen, and D. J. Singh, Phys. Rev. B **50**, 6442 (1994).

[4] L. Vočadlo, G. A. de Wijs, G. Kresse, M. Gillan, and G. D. Price, Faraday Disc. **106**, 205 (1997).

[5] P. Söderlind, J. A. Moriarty, and J. M. Wills, Phys. Rev. B **53**, 14063 (1996).

[6] D. Alfè, G. Kresse, and M. J. Gillan, Phys. Rev. B **61**, 132 (2000).

[7] L. Vočadlo, J. Brodholt, D. Alfè, M. J. Gillan, and G. D. Price, Phys. Earth Planet. Interiors **120**, 145 (2000).

[8] G. A. de Wijs, G. Kresse, L. Vočadlo, D. Dobson, D. Alfè, M. J. Gillan, and G. D. Price, Nature (London) **392**, 805 (1998).

[9] K. Staliunas, Phys. Rev. Lett. **81**, (1998).

[10] D. Alfè, M. J. Gillan, and G. D. Price, Nature (London) **401**, 462 (1999).

[11] D. Alfè, G. D. Price, and M. J. Gillan, Phys. Rev. B **65**, 165118 (2002).

[12] D. Alfè, Phys. Rev. B **79**, 060101 (2009).

[13] E. Sola, J. P. Brodholt, and D. Alfè, Phys. Rev. B **79**, 024107 (2009).

[14] E. Sola and D. Alfè, Phys. Rev. Lett. **103**, 078501 (2009).

[15] X. Sha and R. E. Cohen, J. Phys. Condens. Matter **23**, 075401 (2011).

[16] R. Kubo, J. Phys. Soc. Jpn. **12**, 570 (1957).

[17] D. A. Greenwod, Proc. Phys. Soc. **71**, 585 (1958).

[18] P. L. Silvestrelli, A. Alavi, and M. Parrinello, Phys. Rev. B **55**, 15515 (1997).

[19] F. Knider, J. Hugel, and A. V. Postnikov, J. Phys. Condens. Matter **19**, 196105 (2007).

[20] M. Pozzo, M. P. Desjarlais, and D. Alfè, Phys. Rev. B **84**, 054203 (2011).

[21] P. L. Silvestrelli, Phys. Rev. B **60**, 16382 (1999).

[22] M. P. Desjarlais, J. D. Kress, and L. A. Collins, Phys. Rev. E **66**, 025401 (2002).

[23] V. Recoules and J-P. Crocombette, Phys. Rev. B **72**, 104202 (2005).

[24] A. Kietzmann, B. Holst, R. Redmer, M. P. Desjarlais, and T. R. Mattsson, Phys. Rev. Lett. **98**, 190602 (2007).

[25] B. Holst, R. Redmer, and M. P. Desjarlais, Phys. Rev. B **77**, 184201 (2008).

[26] D. E. Hanson, L. A. Collins, J. D. Kress, and M. P. Desjarlais, Phys. Plasmas **18**, 082704 (2011).

[27] T. R. Mattsson and M. P. Desjarlais, Phys. Rev. Lett. **97**, 017801 (2006).

[28] Y. Wang and J. P. Perdew, Phys. Rev. B **44**, 13298 (1991); J. P. Perdew, J. A. Chevary, S. H. Vosko, K. A. Jackson, M. R. Pederson, D. J. Singh, and C. Fiolhais, *ibid.* **46**, 6671 (1992).

[29] A. L. Wysocki, R. F. Sabirianov, M. van Schilfgaarde, and K. D. Belashchenko, Phys. Rev. B **80**, 224423 (2009).

[30] N. F. Mott, Proc. R. Soc. London A **153**, 699 (1936).

[31] A. H. Wilson, Proc. R. Soc. London A **167**, 580 (1938).

[32] R. J. Weiss and A. S. Marotta, J. Phys. Chem. Solids **9**, 302 (1959).

[33] N. G. Bäcklund, J. Phys. Chem. Solids **20**, 1 (1961).

[34] G. Kresse and J. Furthmuller, Comp. Mater. Sci. **6**, 15 (1996).

[35] P. E. Blöchl, Phys. Rev. B **50**, 17953 (1994).

[36] G. Kresse and D. Joubert, Phys. Rev. B **59**, 1758 (1999).

[37] J. P. Perdew and A. Zunger, Phys. Rev. B **23**, 5040 (1981).

[38] S. H. Vosko, L. Wilk, and M. Nusair, Can. J. Phys. **58**, 1200 (1980).

[39] D. Alfè, Comp. Phys. Comm. **118**, 31 (1999).

[40] H. C. Andersen, J. Chem. Phys. **72**, 2384 (1980).

[41] H. J. Monkhorst and J. D. Pack, Phys. Rev. B **13**, 5188 (1976).

[42] A. Baldereschi, Phys. Rev. B **7**, 5212 (1973).